CD151 Gene Delivery Activates PI3K/Akt Pathway and Promotes Neovascularization after Myocardial Infarction in Rats

Zhenzhong Zheng, Zhengxiang Liu

Department of Cardiology of Tongji Hospital, Tongji Medical College, Huazhong University of Science and Technology, Wuhan, People's Republic of China

Our previous study showed that CD151 promotes neovascularization and improves blood perfusion in a rat hindlimb ischemia model. In this study, we investigated whether CD151 promotes neovascularization and improves ventricular function after myocardial infarction in rats and the mechanisms involved. Rats were subjected to sham surgery or coronary artery ligation. We used rAAV for direct delivery of the human CD151 gene into the rat myocardium. At 4 weeks after coronary artery ligation, human CD151 mRNA was detected using RT-PCR. Measurement of capillary density was evaluated using immunostaining for von Willebrand factor, and hemodynamic variables and physiological parameters were monitored. Western blot analysis for CD151, PI3K, phosphor-Akt, total Akt, phosphor-eNOS, and total eNOS was performed. In addition, we also observed the effect of CD151 on the expression of VEGF using Western blot analysis. CD151 gene delivery could increase the expression of CD151 at gene and protein levels. Overexpression of CD151 could increase the number of microvessels in the ischemic myocardium and significantly improved the hemodynamic variables after myocardial infarction. In addition, CD151 could activate the PI3K pathway, including activation of Akt and eNOS, but did not affect the expression of VEGF. This study suggested that CD151 could promote neovascularization and improve ventricular function after myocardial infarction in rats. The mechanism may be that CD151 can activate the PI3K pathway and promote neovascularization via the PI3K pathway, without affecting ischemia-induced VEGF expression.

Online address: http://www.molmed.org
doi: 10.2119/2006-00037.Zheng

INTRODUCTION

Therapeutic angiogenesis may be beneficial in the treatment of ischemia, as has recently been substantiated by a large amount of experimental data. Ischemic heart diseases develop as a consequence of coronary atherosclerotic lesion formation. Coronary collateral vessels and microvascular angiogenesis, which ameliorate the function of the damaged heart, develop as an adaptive response to myocardial ischemia. Previous studies have shown that CD151-induced formation of cord-like structures on matrigel is an in vitro model of angiogenesis. In addition, CD151 antibody inhibition of cord-like structures on matrigel seen in NIH3T3 cells was confirmed using HUVECs, suggesting that CD151 may contribute to angiogenesis (1,2). Our research has revealed that CD151 promotes neovascularization and angiogenesis, which suggests that CD151 is a potential therapeutic reagent for treating ischemia by inducing angiogenesis (3). Whether CD151 promotes neovascularization and angiogenesis after myocardial infarction in rats is still unclear, however; the precise molecular mechanisms responsible for the function of CD151 are still poorly defined, and the signaling pathways involved need to be better defined.

Many growth factors and hormones have been shown to exert their cellular functions, including the activation of eNOS activity, via the PI3K/Akt signaling pathway (4). We hypothesized that CD151 may activate the PI3K/Akt pathway and affect angiogenesis. Recombinant adeno-associated virus (rAAV) presents several biological properties that render it suitable as a vector for long-term expression of therapeutic genes. The virus is nonpathogenic and elicits an attenuated host inflammatory response. In addition, rAAV has tropism for many mammalian cell types and has the capacity for integration into the host genome, thereby permitting prolonged expression of the transgene (5). To test whether CD151 promotes neovascularization and angiogenesis after myocardial infarction, we used rAAV for direct delivery of the human CD151 gene into the rat myocardium, evaluating the effect of CD151 on the PI3K pathway and neovascularization. Therefore, the purpose of this study was to determine the mechanisms by which CD151 promotes neovascularization after myocardial infarction.

MATERIALS AND METHODS

Preparation of rAAV-CD151 and rAAV-GFP

The rAAV vector plasmid, the adenovirus helper plasmid pXX6, and the packaging plasmid pXX2 have been described (3,6). Briefly, dsAAV-CD151 and dsAAV-GFP vector plasmids were constructed by inserting the human CD151 cDNA and GFP cDNA, respectively, into the rAAV vector driven by cytomegalovirus (CMV) promoter. The vec-

Address correspondence and reprint requests to *Zhengxiang Liu, Department of Cardiology, Tongji Hospital, Tongji Medical College, Huazhong University of Science and Technology, 1095 JieFang Avenue, Wuhan 430030 China. Fax: 86-027-83662622; e-mail: liuzhengxiang@hotmail.com*

Submitted May 20, 2006; accepted for publication September 6, 2006.

tors for rAAV-CD151 and rAAV-GFP were prepared using a triple-plasmid cotransfection method in 293 cell lines, as described (7). A total of 85 μg of plasmid DNA per 15-cm plate (dsAAV-CD151 or dsAAV-GFP/pXX2/pXX6 in 1:1:1 molar ratios) were used for transfection. In large-scale rAAV preparations, a single-step gravity-flow column purification method was carried out as described (8). The eluted rAAV was divided into aliquots and stored at –80°C.

To measure the titer of rAAV vectors, 5 μL rAAV vector was digested with 5 units DNase I at 37°C for 1 h followed by digestion with 100 μg proteinase K in proteinase K buffer for 1 h at 37°C. The reaction was then extracted with an equal volume of phenol/chloroform/isoamyl alcohol, and the titer of rAAV-CD151 and rAAV-GFP was determined by quantitative real-time PCR (Realtime PCR Master Mix, Japan) (9).

Myocardial Infarction and Intramyocardial Gene Delivery

Rats (Animal Apply Center, Tongji Medical College, Wuhan, China) weighing 200-250 g were randomly divided into 4 groups and subjected to sham surgery or coronary artery ligation. Under pentobarbital anesthesia (60 mg/kg intraperitoneally), acute myocardial infarction (AMI) was induced by ligation of the left anterior descending coronary artery. Briefly, after intubation of the trachea an incision was made in the skin overlying the 4th intercostal space, with the overlying muscles separated and kept aside. The animals were put on positive-pressure ventilation (frequency 65–70/min, tidal volume 3 mL), and the thoracic cavity was opened by cutting the intercostal muscles. The heart was carefully pushed to the left, and 6.0 silk suture was looped under the left descending coronary artery near the origin of the pulmonary artery. Proper occlusion of the coronary artery resulted in an extensive transmural infarction comprising a major part of the LV free wall, with small variations in size. Coronary occlusion was confirmed by the presence of deep S waves on the electrocardiogram (ECG) and ventricular arrhythmias within the 1st 20-30 min after occlusion.

Rats with myocardial infarction were assigned to groups treated with saline (AMI + saline), rAAV-GFP (AMI + rAAV-GFP), or rAAV-CD151 (AMI + rAAV-CD151). Sham-operated animals underwent the same surgical procedure without the coronary artery ligation. For direct gene delivery, 4×10^{11} particles of rAAV-CD151 vector were delivered subepicardially with a curved 25-gauge needle into 5 sites along the region of the myocardium supplied by the left ascending coronary artery (LAD). Sham-operated animals and AMI control animals received an equivalent volume of either sterile Ringer's saline or 4×10^{11} particles of rAAV-GFP. After returning the heart to its normal position, the suture was tied. The intercostal space was closed by pulling the ribs with 3.0 silk, the muscles were returned to their normal position, the skin incision was sutured, and the animals were allowed to recover. All experiments were conducted in accordance with the institutional guidelines for animal research and conform with the *Guide for the Care and Use of Laboratory Animals* published by the US National Institutes of Health (NIH publ. no. 85-23, revised 1996).

RT-PCR Analysis

At 4 weeks after coronary artery ligation, RNA was extracted from fresh rat tissues from the ischemic area using Trizol (Gibco), according to the manufacturer's instructions. Human ECV304 cells (human umbilical vein endothelial cell line) were purchased from China Center for Type Culture Collection (China) and cultured in DMEM supplemented with 10% FBS, penicillin, and streptomycin. ECV304 cells transfected with rAAV-CD151 were used as positive control. RT-PCR analysis specific for human CD151 (forward primer, 5′-GAGGTCTATG GGTGAGTTCAACGAG-3′; reverse primer, 5′-AATTCCTCAGGCGTAGTC-3′) and β-actin (forward primer, 5′-GGAGA AGGACCCAGATC-3′; reverse primer, 5′-GATCTTCATGAGGTAGTCAG-3′) was then performed using the RT-PCR kit (Takara Biotechnology) according to the manufacturer's instructions.

Western Blot Analysis

Tissue samples from the infarcted area of 3 to 5 rats per group were dissected. The tissues were homogenized in 500 μL of 25 mmol/L Tris-HCl (pH 7.4) containing 1% Triton X-100, 0.1% SDS, 2 mmol/L EDTA, and 1% protease inhibitor cocktail (Sigma) and centrifuged at 14000*g* for 30 min at 4°C. The supernatants were used for Western blot analysis, with specific antibodies detecting CD151 (Serotec, UK), PI3K (p110), phosphor-Akt^{473}, total Akt, phosphor-eNOS^{1177}, total eNOS, and VEGF (Santa Cruz, CA, USA). According to standard protocols, the blots were probed with various primary antibodies, and the HRP-conjugated secondary antibodies were used to reveal the specific protein bands with ECL detection reagents. The intensities of the various protein bands were quantified by densitometry.

Measurement of Capillary Density

Blood vessels were highlighted by immunostaining for von Willebrand factor (vWF) (Invitrogen), visualized with diaminobenzidine (DAB). In brief, the hearts were fixed in 10% neutral-buffered formaldehyde for 12 h and embedded in paraffin, cut into 5-μm sections, and deparaffinized with a graded series of xylene and ethanol solutions. Sections were deparaffinized and microwave-treated for 10 min twice in 10 mM sodium citrate (pH 6.0). Endogenous peroxidase in the section was blocked by incubating them in endogenous peroxidase blocking solution for 10 min at room temperature. A rabbit polyclonal antibody against vWF protein was used as primary antibody in a 1:70 dilution at 4°C for 18 h. After washing 3 times with PBS, sections were incubated with biotin-conjugated anti-rabbit secondary antibody for 10 min. They were then washed 3 times with PBS, treated with streptavidin-peroxidase for 10 min, and washed again with PBS 3 times. Fi-

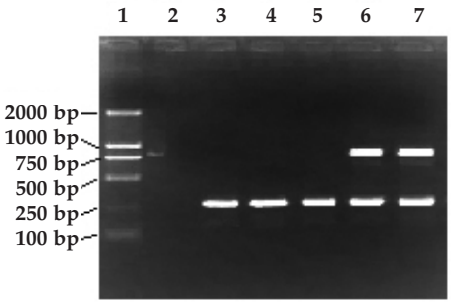

Figure 1. Detection of human CD151 gene expression by RT-PCR. RT-PCR was performed using 5 μg total RNA and a pair of oligonucleotide primers specific to human CD151. The anticipated sizes of PCR products for CD151 and β-actin were 799 and 300 bp, respectively. The RNA extracted from ECV304 transfected with rAAV-CD151 was used as a positive control (lane 7). The human CD151mRNA was detected in ischemic myocardium (lane 6), but not in the other groups (lane 3, sham; lane 4, AMI + saline; lane 5, AMI + rAAV-GFP). Double-distilled water was used as a negative control (lane 2).

nally, specimens were incubated in DAB for 5 min, followed by hematoxylin counterstaining. The density of capillaries in each field was evaluated by counting vessels in a total of 5 high-power fields (magnification ×400) per region per heart under ocular micrometers (Olympus).

Hemodynamic Variables and Physiological Parameters

Under pentobarbital anesthesia, hemodynamic variables were monitored using a catheter tip manometer (AD Instruments) advanced from the right carotid artery via the aortic arch into the left ventricle (LV), providing parameters of global ventricular function such as left ventricular end-diastolic pressure (LVEDP), left ventricle end-systolic pressure (LVESP), and the maximal-minimum rate of LVP ($\pm dp/dt_{max}$) were measured and evaluated. All values were acquired in repeated heart cycles, and for an individual heart, each value was expressed as the mean of 5 cardiac cycles/time point.

The animals were anesthetized with pentobarbital and the hearts were removed. The whole heart and left ventricle were then weighed. The interventricular septum was included in the left ventricular weight. Left ventricle/body weight and whole heart/body weight were calculated.

Statistical Analysis

Data were expressed as mean ± SEM. Comparisons of parameters among the 4 groups were performed by 1-way ANOVA, followed by Newman-Keuls test for unpaired data. Comparisons of parameters between 2 groups were made by unpaired Student *t* test. *P* values of < 0.05 were considered statistically significant.

RESULTS

CD151 Gene Delivery Increases the Expression of Human CD151 mRNA and Protein

Human CD151 mRNA was detected in the hearts of the AMI + rAAV-CD151 group and the ECV304 cells transfected with rAAV-CD151 (positive control), but not in the other group that received rAAV-GFP or saline (Figure 1). Similar levels of β-actin mRNA were detected in all tested tissues, confirming the integrity of prepared RNA.

The expression of CD151 protein was increased significantly ($P < 0.05$) in the AMI + rAAV-CD151 group compared with other groups (Figure 2). There was no significant ($P > 0.05$) difference of the expression of CD151 between the AMI + rAAV-GFP, AMI + rAAV-saline, and sham-operated groups. The results indicated that rAAV-CD151 administration could promote CD151 protein expression, which confirmed that rAAV-mediated gene transfer could drive stable long-term expression of the CD151 gene in vivo.

Analysis of Capillary Density

Immunohistochemical staining for vWF showed higher microvessel densities in the AMI + rAAV-CD151 group and less neovascularization in the AMI + rAAV-saline or AMI + rAAV-GFP groups

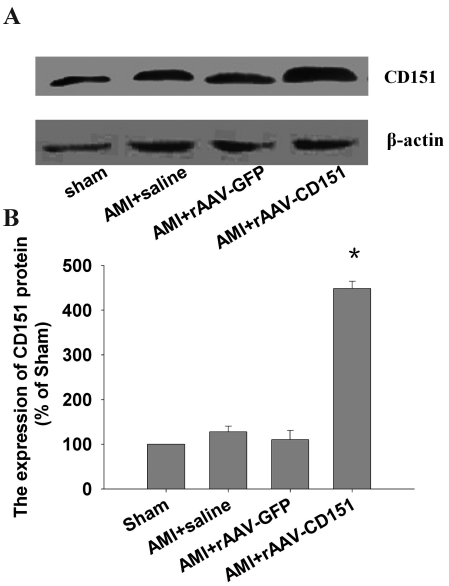

Figure 2. The expression of CD151 after CD151 gene delivery. Four weeks after coronary artery ligation, samples were taken from the same regions as the ischemic heart. (A) Western blot analysis for CD151 and β-actin in hearts of different groups. β-Actin was used as an internal loading control. (B) Quantitative results of CD151. The mean density of CD151 in sham-operated mice was defined as 100%. Data are means ± SEM (n = 6-8). *$P < 0.05$ vs. sham, AMI + saline, AMI + rAAV-GFP.

(Figure 3A). Hearts of the sham-operated group were relatively avascular. The densities of total microvessels were higher in the AMI + rAAV-CD151 group than in the AMI + rAAV-saline or AMI + rAAV-GFP groups (Figure 3B). There were no significant differences ($P > 0.05$) between the AMI + rAAV-saline group and the AMI + rAAV-GFP group—the number of microvessels was similar between the groups.

Hemodynamic Variables and Physiological Parameters

There were significant ($P < 0.05$) differences observed in hemodynamics between the AMI + rAAV-CD151 group and the other groups (Table 1). The cardiac function in AMI was markedly deteriorated compared with sham-operated

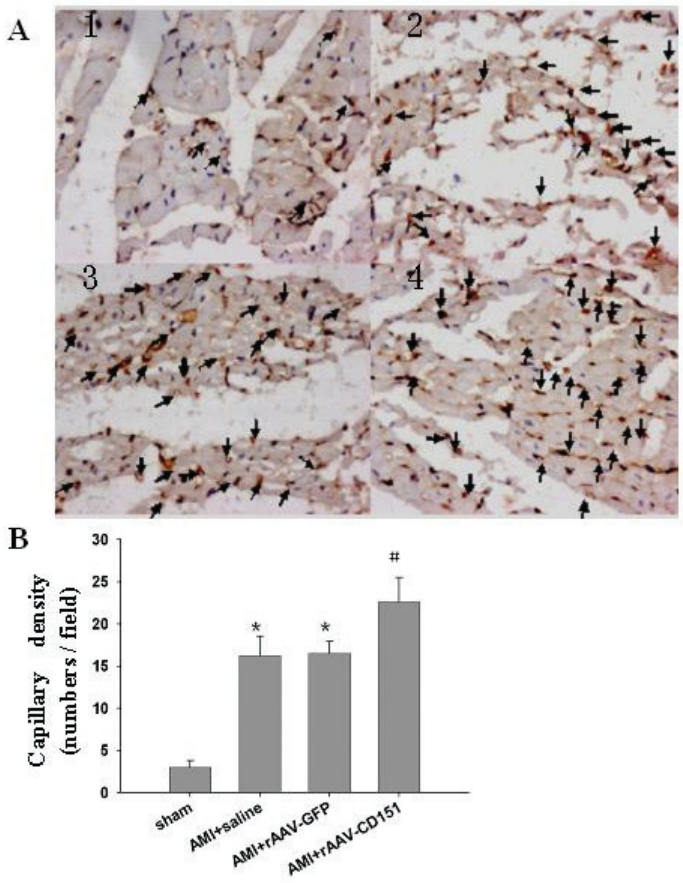

Figure 3. Analysis of capillary density. Hearts of the sham group were relatively avascular. (A) Hearts transfected with rAAV-GFP and injected with physiological saline had greater capillary density, and vascular densities were highest in hearts transfected with rAAV-CD151. The arrows indicate the endothelial cells stained positive with vWF (1, sham; 2, AMI + saline; 3, AMI + rAAV-GFP; 4, AMI + rAAV-CD151). (B) Myocardial vessel density in ischemic zones of sham, AMI + saline, AMI + rAAV-GFP, and AMI + rAAV-CD151 groups. *P < 0. 05 vs. AMI + saline and AMI + rAAV-GFP. #P < 0. 05 vs. sham.

rats. rAAV-mediated CD151 gene delivery significantly improved the hemodynamic variables, including increase in LVESP and $\pm dp/dt_{max}$ and decrease in LVEDP. These data indicate an improvement in systolic and diastolic functions by rAAV-CD151 treatment.

In addition, we measured the ratio of left ventricular weight/body weight and heart weight/body weight. As shown in Table 1, left ventricular weight/body weight among these groups was not changed at 4 weeks after AMI. However, heart weight/body weight ratios in the AMI + rAAV-CD151 group, AMI + rAAV-saline group, and AMI + rAAV-GFP group were increased compared with the sham group—AMI resulted in an increase in heart weight/body weight. Heart weight/body weight in the AMI + rAAV-CD151 group was reduced compared with the AMI + rAAV-saline group and AMI + rAAV-GFP group after AMI. CD151 gene delivery tended to reduce heart weight/body weight after AMI compared with the AMI + rAAV-saline and AMI + rAAV-GFP groups.

Western Blot Analysis

To test whether CD151 activates the PI3K pathway, Western blots for PI3K, total Akt, total eNOS, phosphor-Akt, and phosphor-eNOS protein were performed 4 weeks after intramyocardial gene delivery.

Table 1. Hemodynamic variables and physiological parameters

Parameter	Sham	AMI + saline	AMI + rAAV–GFP	AMI + rAAV–CD151
n	8	6	6	7
BW, g	341.38 ± 11.61	344.83 ± 11.77	353.67 ± 19.44	343 ± 17.18
LVW, mg	721.3 ± 22.90	755 ± 15.17	746.7 ± 45.46	717.14 ± 22.15
HW, mg	853.25 ± 39.88	1075 ± 94.18	1086.67 ± 127.23	942.57 ± 56.21
LVW/BW, mg/g	2.11 ± 0.07	2.14 ± 0.05	2.13 ± 0.11	2.09 ± 0.07
HW/BW, mg/g	2.50 ± 0.11	3.08 ± 0.29*	3.07 ± 0.25*	2.75 ± 0.08†
LVEDP, mmHg	3.51 ± 0.61	23.27 ± 2.42*	23.3 ± 3.26*	4.89 ± 8.81†
LVESP, mmHg	135.66 ± 2.00	113.5 ± 3.54*	115.20 ± 2.26*	126.11 ± 2.64†
$+dp/dt_{max}$, mmHg/s	7400.75 ± 129.27	3522.33 ± 307.66*	3713 ± 195.53*	6073.29 ± 407.96†
$-dp/dt_{max}$, mmHg/s	4417.13 ± 142.75	3764.83 ± 99.91*	3710.83 ± 170.10*	3992.29 ± 120.60†

At 4 weeks after coronary artery ligation, hemodynamic variables were monitored using a catheter tip manometer advanced from the right carotid artery via the aortic arch into the left ventricle at the end of the experiment. Data represent means ± SEM. BW, body weight; HW, heart weight; LVW, left ventricular weight; LVEDP, left ventricle end–diastolic pressure; LVESP, left ventricle end–systolic pressure; $\pm dp/dt_{max}$, maximal rate of increase and decline in left ventricular pressure. *P < 0. 05 vs. sham; †P < 0.05 vs. sham, AMI + saline, and AMI + rAAV–GFP.

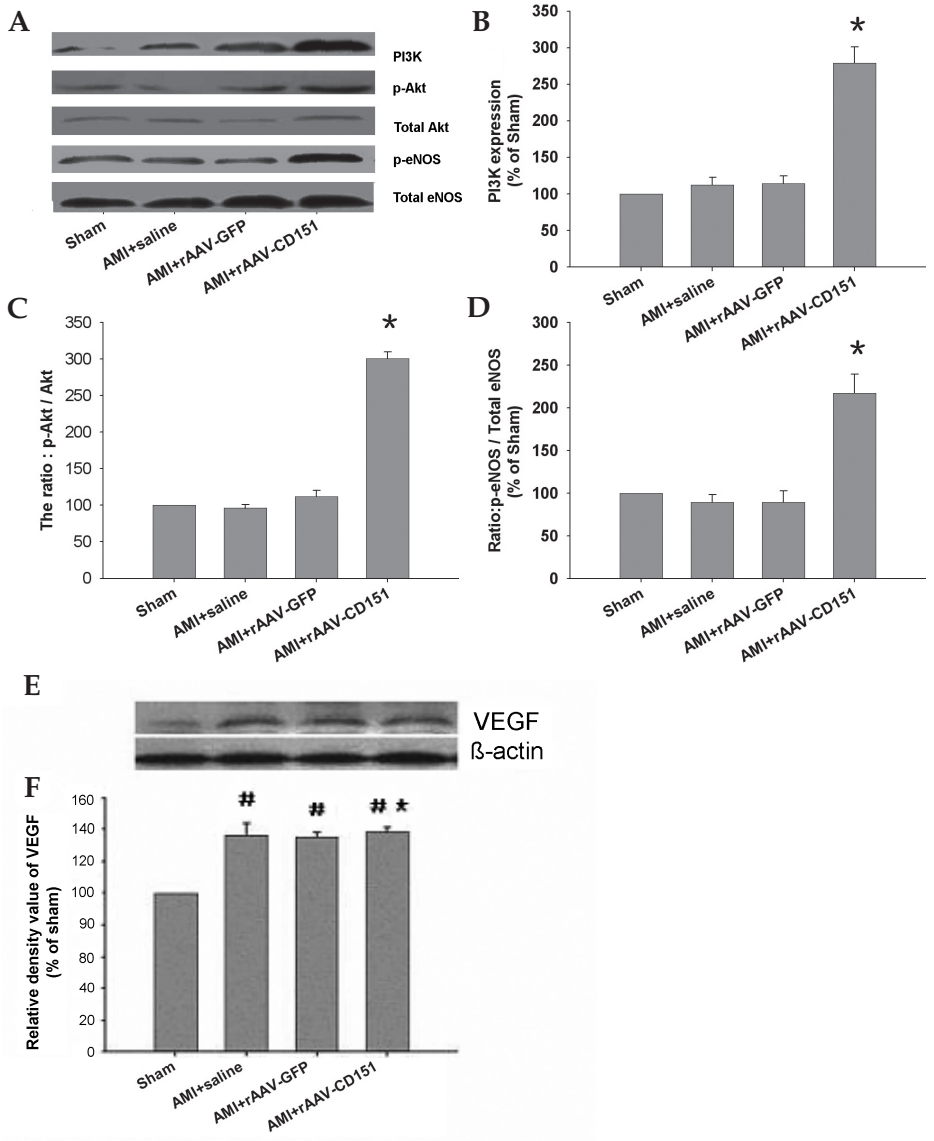

Figure 4. Expression of PI3K, phosphor-Akt, total Akt, phosphor-eNOS, total eNOS, and VEGF after CD151 gene delivery. Four weeks after coronary artery ligation, samples were taken from the same regions as the ischemic heart. (A) Western blot of PI3K, phosphor-Akt, total Akt, phosphor-eNOS, and total eNOS in hearts of different groups. (B, C, D) Quantitative analysis of phosphor-Akt, phosphor-eNOS, total Akt, total eNOS. The mean density of PI3K (B), phosphor-Akt and total Akt (C), and phosphor-eNOS and total eNOS (D) in sham-operated mice was defined as 100%. (E, F) Quantitative analysis of VEGF. The mean density of VEGF in sham-operated mice was defined as 100%. Data are means ± SEM. *$P > 0.05$ vs. AMI + saline, AMI + rAAV-GFP. #$P < 0.05$ vs. sham.

We found that CD151 gene delivery increased the expression of PI3K significantly ($P < 0.05$) in the AMI + rAAV-CD151 group compared with the AMI + rAAV-GFP, AMI + rAAV-saline, and sham-operated groups (Figure 4A,B). There was no significant ($P > 0.05$) difference of the expression of total eNOS and total Akt protein in the 4 groups. When phosphor-Akt and phosphor-eNOS levels were normalized with the expression of Akt and total eNOS protein, respectively, the ratio was increased significantly ($P < 0.05$) in the AMI + rAAV-CD151 group compared with the AMI + rAAV-GFP, AMI + rAAV-saline, and sham-operated groups, whereas there were no significant differences ($P > 0.05$) among the AMI + rAAV-GFP, AMI + rAAV-saline, and sham groups (Figure 4C,D). These results suggest that overexpression of CD151 activates the PI3K pathway and increases phosphorylation of Akt and eNOS, leading to activation of eNOS.

In addition, we detected the expression of VEGF after gene transfection. The expression of VEGF increased significantly ($P < 0.05$) in rats after AMI compared with the sham group, but there were no significant differences ($P > 0.05$) among the rats subjected to sham surgery or coronary artery ligation (Figure 4E,F), which suggests that overexpression of CD151 did not affect the expression of VEGF.

DISCUSSION

Angiogenesis is a complex process involving endothelial cell proliferation, migration, remodeling of extracellular matrix, and formation of tubular structures. Angiogenesis can be quantified by different methods based on the microscopic evaluation of tissue vascularization using antibodies with affinity for specific epitopes on the endothelial cell, such as VEGF, CD31, CD34, and vWF or factor VIII (10-12). According to Tomoda et al. (13) and Sion-Vardy et al. (14), anti-vWF is the antibody of choice in the assessment of angiogenesis, so the expression of vWF was evaluated in the present study. Our observation showed that delivery of the CD151 gene increased capillary density after AMI in rats, which is consistent with our hypothesis.

Previous studies have shown that Akt is a serine/threonine protein kinase that is recruited to the membrane by its binding to PI3K-produced phosphoinositides. At the membrane, Akt is phosphorylated and activated by phosphoinositide-dependent kinases (4,15). Akt subsequently phosphorylates and activates eNOS. Formation of NO has been found

to occur after activation of PI3K and Akt, which phosphorylates eNOS (16,17). eNOS, and its subsequent product, NO, has a crucial role in the regulation of vascular tone, vascular remodeling, and angiogenesis (18-20). In the present study, we showed that CD151 gene delivery increased the expression of CD151 protein; at the same time the expression of PI3K, phosphorylation of Akt, and phosphorylation of eNOS protein increased as well, but the total Akt and eNOS had no change in the 4 groups, which indicated that CD151 could activate the PI3K pathway, leading to activation of Akt and eNOS via phosphorylation, and increase the activity of eNOS. Studies have shown that ischemia acts as a stimulus for eNOS activation, resulting in increased eNOS activity and increased NO release (21). We found increased capillary density induced by AMI, but we were unable to detect any difference in increases in phosphorylated Akt and eNOS in the rAAV-GFP or saline groups compared with the sham group. The reason for this discrepancy remains enigmatic.

Numerous molecules have been reported to take part in the process of angiogenesis. VEGF is considered one of the most important growth factors in angiogenesis (22). Previous studies have demonstrated that the endothelial cell mitogen VEGF promotes neovascularization in vitro and in vivo (23,24). To determine whether VEGF is involved in the angiogenic effect of CD151, we measured VEGF expression after gene transfer. In ischemic rat myocardium, the increased VEGF levels could contribute to coronary microvascular density after MI, and the increased VEGF levels could promote angiogenesis. The induction of VEGF expression might explain the principal mechanism in VEGF's role in ischemia-induced in vivo angiogenesis. Interestingly, there was no significant change in VEGF expression of animals treated with rAAV-CD151 compared with other animals with myocardial infarction, which indicated that rAAV-CD151 gene transfer did not affect VEGF protein levels. These results indicate that CD151-induced angiogenesis is not mediated by VEGF. Our present study demonstrated that activation of the PI3K pathway by CD151 augments neovascularization in ischemic myocardium without affecting ischemia-induced VEGF expression following MI after CD151 gene delivery. The mechanisms by which CD151 affects the PI3K pathway and angiogenesis are unknown at present. The most likely hypothesis is that CD151 can function as a transmembrane linker interacting with proteins regulating the PI3K/Akt pathway.

In addition, the present study showed that $\pm dp/dt_{max}$ was increased in the AMI + rAAV-CD151 group. Systolic contractility, assessed as LVESP, tended to improve after CD151 gene delivery. Diastolic relaxation, as determined by LVEDP, was improved after underpacing conditions, too. rAAV-mediated CD151 gene delivery significantly improved the hemodynamic variables, the possible mechanisms being (1) increase in capillary density or (2) inhibitory heart remodeling—CD151 gene delivery tended to reduce heart weight/body weight after AMI. After myocardial infarction, ventricular remodeling occurs in both the myocardium surrounding the infarcted tissue (border zone) and the myocardium remote from the infarct to preserve cardiac output and limit wall stress. The activation of the PI3K/Akt pathway by CD151 leads to phosphorylation of eNOS. NO derived from eNOS can modulate many of the processes leading to ventricular remodeling. In clinical studies, long-term administration of nitrates (NO-donor compounds) limited LV remodeling after MI (25). NO causes systemic vascular relaxation (26), thereby reducing cardiac preload and afterload. Much evidence suggests that NO can increase angiogenesis (27), decrease cardiac fibrosis (28), and decrease angiotensin II–induced cardiac myocyte hypertrophy (29), all of which could limit ventricular remodeling after MI.

Our findings also indicate that rAAV is an efficient vector for in vivo transfer and sustained expression of therapeutic genes into the myocardium and that rAAV-mediated CD151 gene transfer provides effective and long-lasting protection from AMI-induced myocardial injury.

In summary, we extend our previous findings, demonstrating that CD151 activates the PI3K/Akt pathway, induces neovascularization and angiogenesis, and improves ventricular function after myocardial infarction in rats. To our knowledge, this is the first documentation that CD151 promotes neovascularization in the postinfarcted heart. The preliminary data, although very encouraging, need to be well discussed and further study surely continued. It is possible that further study of CD151 will provide clues for better understanding its function and may help uncover novel therapeutic strategies for regulating the angiogenic process.

ACKNOWLEDGMENTS

We are grateful to Dr. Xin Zhang for providing PzeoSV-CD151 plasmid (Department of Molecular Science, University of Tennessee Health Science Center, USA). We are also grateful to Dr. Xiao Xiao for providing us with dsAAV-GFP, PXX2, PXX6 (University of Pittsburgh, PA, USA). We also thank the expert technical assistance of Pro. Daowen Wang and his students Yong Wang and Yan Wang.

This work was supported by a grant from the Nature Science Foundation of China (no. 30570728) and the Science Research Foundation of Health Department of Hubei province (no. JX2A04)

REFERENCES

1. Fitter S, Sincock PM, Jolliffe CN, Ashman LK. (1999) Transmembrane 4 superfamily protein CD151 (PETA-3) associates with β1 and αIIb β3 integrins in hemopoietic cell lines and modulates cell-cell adhesion. *Biochem. J.* 15:61-70.
2. Zhang XA, Kazarov AR, Yang X, Bontrager AL, Stipp CS, Hemler ME. (2002) Function of the tetraspanin CD151-$\alpha_6\beta_1$ integrin complex during cellular morphogenesis. *Mol. Biol. Cell* 13:1–11.
3. Lan RF, Liu ZX, Liu XC, Song YE, Wang DW. (2005) CD151 promotes neovascularization and improves blood perfusion in a rat hind-limb ischemia model. *J. Endovasc. Ther.* 12:469-78.

4. Datta SR, Brunet A, Greenberg ME. (1999) Cellular survival: a play in 3 Akts. *Genes Dev.* 13:2905-27.
5. Flotte TR, Carter BJ. (1995) Adeno-associated virus vectors for gene therapy. *Gene Ther.* 2:357-62.
6. Lan R, Liu Z, Song Y, Zhang X. (2004) Effects of rAAV-CD151 and rAAV-antiCD151 on the migration of human tongue squamous carcinoma cell line Tca8113. *J. Huazhong. Univ. Sci. Technol. Med. Sci.* 24:556-9.
7. Xiao X, Li J, Samulski RJ. (1998) Production of high-titer recombinant adeno-associated virus vectors in the absence of helper adenovirus. *J. Virol.* 72:2224-32.
8. Auricchio A, Hildinger M, O'Connor E, Gao GP, Wilson JM. (2001) Isolation of highly infectious and pure adeno-associated virus type 2 vectors with a single-step gravity-flow column. *Hum. Gene Ther.* 12:71-6.
9. Rohr UP, Wulf MA, Stahn S, Steidl U, Haas R, Kronenwett R. (2002) Fast and reliable titration of recombinant adeno-associated virus type-2 using quantitative real-time PCR. *J. Virol. Methods* 106:81-8.
10. Maeda KS, Chung Y-S, Takatsuka S. (1995) Tumour angiogenesis and tumor cell proliferation as prognostic indicators in gastric carcinoma. *Br. J. Cancer* 72:319-23.
11. Pazouki S et al. (1997) The association between tumor progression and vascularity in the oral mucosa. *J. Pathol.* 183:39-43.
12. Weidner N, Sample JP, Welch WR. (1991) Tumor angiogenesis and metastasis: correlation in invasive breast carcinoma. *N. Engl. J. Med.* 324:1-8.
13. Tomoda M et al. (1999) Intratumoral neovascularization and growth pattern in early gastric carcinoma. *Cancer* 85:2340-6.
14. Sion-Vardy N, Liss DM, Prints-Loo I, Shoham-Vardi I, Benharroch D. (2001) Neoangiogenesis in squamous cell carcinoma of the larynx: biological and prognostic associations. *Pathol. Res. Pract.* 197:1-5.
15. Toker A, Newton AC. (2000) Akt/protein kinase B is regulated by autophosphorylation at the hypothetical PDK-2 site. *J. Biol. Chem.* 275:8271-4.
16. Dimmeler S, Fleming I, Fisslthaler B, Hermann C, Busse R, Zeiher AM. (1999) Activation of nitric oxide synthase in endothelial cells by Akt-dependent phosphorylation. *Nature* 399:601-5.
17. Fulton D et al. (1999) Regulation of endothelium-derived nitric oxide production by the protein kinase Akt. *Nature* 399:597-601.
18. Zhao X, Lu X, Feng Q. (2002) Deficiency in endothelial nitric oxide synthase impairs myocardial angiogenesis. *Am. J. Physiol. Heart. Circ. Physiol.* 283:H2371-8.
19. Morbidelli L, Donnini S, Ziche M. (2004) Role of nitric oxide in tumor angiogenesis. *Cancer Treat. Res.* 117:155-67.
20. Isenberg JS. (2004) Nitric oxide modulation of early angiogenesis. *Microsurgery* 24:385-91.
21. Bloch W, Mehlhorn U, Krahwinkel A, Reiner M. (2001) Ischemia increases detectable endothelial nitric oxide synthase in rat and human myocardium. *Nitric Oxide* 5:317-33.
22. Ferrara N, Gerber HP, LeCouter J. (2003) The biology of VEGF and its receptors. *Nat. Med.* 9:669-76.
23. Nicosia RF, Nicosia SV, Smith M. (1994) Vascular endothelial growth factor, platelet-derived growth factor, and insulin-like growth factor-1 promote rat aortic angiogenesis in vitro. *Am. J. Pathol.* 145:1023-9.
24. Pearlman JM et al. (1995) Magnetic resonance mapping demonstrates benefits of VEGF-induced myocardial angiogenesis. *Nat. Med.* 1:1085-9.
25. Gruppo Italiano per lo Studio della Sopravvivenza nell'infarcto Miocardico. (1994) GISSI-3: effects of lisinopril and transdermal glyceryl trinitrate singly and together on 6-week mortality and ventricular function after acute myocardial infarction. *Lancet* 343:1115–22.
26. Furchgott RF, Zawadzki JV. (1980) The obligatory role of endothelial cells in the relaxation of arterial smooth muscle by acetylcholine. *Nature* 288: 373-6.
27 Murohara T et al. (1998) Nitric oxide synthase modulates angiogenesis in response to tissue ischemia. *J. Clin. Invest.* 101:2567-78.
28. Kim NN et al. (1999) Regulation of cardiac fibroblast extracellular matrix production by bradykinin and nitric oxide. *J. Mol. Cell. Cardiol.* 31:457-66.
29. Ritchie RH et al. (1998) Angiotensin II-induced hypertrophy of adult rat cardiomyocytes is blocked by nitric oxide. *Am. J. Physiol.* 275:H1370-4.